

Handover Management Based on Location Based Services in F-HMIPv6 Networks

Heba Nashaat, and Rawya Rizk*

Electrical Engineering Department, Port Said University, Port Said, 42523, Egypt
hebanashaat@eng.psu.edu.eg, r.rizk@eng.psu.edu.eg

*Corresponding author: Rawya Rizk

*Received February 13, 2015; revised September 18, 2015; accepted October 13, 2015;
published December 31, 2015*

Abstract

In this paper, a new mathematical scheme of Macro Handover Management (MHM) in F-HMIPv6 networks based on Location Based Services (LBS) is proposed. Previous schemes based on F-HMIPv6 protocol usually suffer from three major drawbacks: First, They don't exploit the information about the user mobility behavior in order to reduce handover effects. Second, they only focus on the micro mobility level. Third, they don't consider the quality of service (QoS) of the traffic. The proposed MHM scheme avoids these drawbacks using the available information about Mobile Node (MN) such as user mobility patterns and MN's velocity to predict handover and improve network's QoS. It also takes the traffic type in consideration since it presents a major factor in locating QoS for the user. MHM is analyzed and compared with the F-HMIPv6. The results show that MHM improves the performance in terms of packet delivery cost, location update cost, and handover latency. The design of MHM comprises software package in the MN in addition to a hardware part in the network side. It has implications for communication, design, and pricing of mobile services.

Keywords: F-HMIPv6, location based service, macro handover, mobility management, mobility prediction.

1. Introduction

MOBILITY management is an essential technology for keeping track of the users' current location and for delivering data correctly [1, 2]. Location Based Services (LBS) in mobile phone has become one of the most important features of communication systems because of its multiple applications. It is a wireless-IP service that uses geographic information to serve a mobile user and enlarge the scope of mobile applications [3].

The Internet Engineering Task Force (IETF) has proposed Mobile IPv6 (MIPv6) [4, 5] as the main protocol for mobility management at the IP layer. Several extensions such as Fast Handovers for MIPv6 (FMIPv6) [6] and Hierarchical MIPv6 (HMIPv6) [7], have been proposed to enhance MIPv6. Combination of HMIPv6 and FMIPv6 motivates the design of Fast Handover for Hierarchical Mobile IPv6 (F-HMIPv6) protocol [8]. It combines more efficient network bandwidth usage of HMIPv6 and the less handover latency and packet loss of FMIPv6.

Fig. 1 shows the network model of F-HMIPv6. A domain is managed by Mobility Anchor Point (MAP). Two MAPs are shown in the figure, Previous MAP (MAP_p) and New MAP (MAP_N). While entering a MAP domain, the mobile node (MN) receives router advertisements containing information about local MAPs from Access Routers (ARs) within range. The MN obtains two care of addresses (CoAs): an onlink Local CoA (LCoA) and a Regional CoA (RCoA) within the selected MAP domain. Then, a Local Binding Update (LBU) message is sent to the MAP to bind the MN's LCoA with its RCoA. Upon receipt of a successful Binding Acknowledgment (BA), the MN updates the binding of its RCoA with the home agent (HA) and each corresponding node (CN). As a result, packets destined to the MN are intercepted by the MAP, encapsulated and forwarded to the MN's onlink address. A movement within the MAP domain (intra domain) merely incurs LBUs at the MAP without further propagation to the HA and CNs. Thus, it significantly reduces the signaling load and micro-mobility handover delays. F-HMIPv6 is an effective integration that has been designed to enable a MN to exchange handover signaling messages with a local MAP. In addition it establishes a tunnel between MAP_p and New AR (NAR_p) in this MAP instead of between the Previous AR (PAR_p) in this MAP and NAR_p [8]. Similarly the same technique is performed in MAP_N and its associated NAR_N and PAR_N .

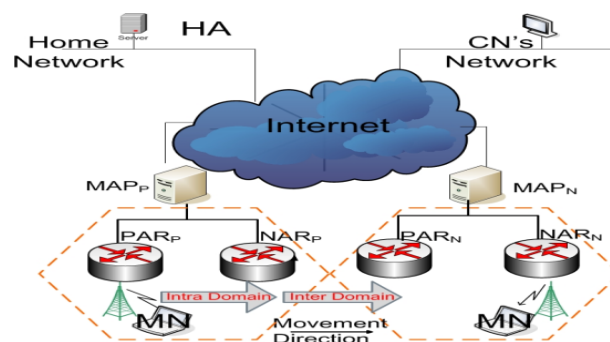


Fig. 1. Network Model of F-HMIPv6.

A number of studies for performance analysis of IPv6 mobility management protocols have been presented. In [9], an analytical model is derived to evaluate the packet loss and packet delivery for UDP streams and the throughput for TCP streams involved in smooth handover for MIPv6. In [10], a general framework of handover management in MIPv6 for video traffic is presented. An analytical model focuses on the effect of Frame Error Rate on the handover latency. In [11], an analytic model to evaluate the performance for HMIP, Dynamic HMIP (DHMIP), and Multicast HMIP (MHMIP) is proposed. In [12], an analytical cost model is developed for evaluating the performance of Proxy MIPv6 (PMIPv6). Analysis and comparison between PMIPv6 and FPMIPv6 are presented in [13].

In [14], the performance analysis of F-HMIPv6 using an analytical model is presented. Location update cost, packet delivery cost and total cost are formulated based on the fluid-flow mobility model. The impact of several wireless system factors are investigated, such as user velocity, user density, mobility domain size, and session-to-mobility ratio. Based on this analytical model, [15] introduces a comprehensive F-HMIPv6 performance analysis for random walk, fluid-flow and Baumann mobility model.

Some literatures introduce analytical comparison between MIPv6, FMIPv6, HMIPv6, and a combination of FMIPv6 and HMIPv6 [16, 17]. A number of studies for enhancement of F-HMIPv6 have been introduced. Enhanced Scheme of F-HMIPv6 (ES-FHMIPv6) is presented in [18]. In [19], a high priority in using hierarchical setup with fast handover is attributed.

Most of the available work in the aspect of performance evaluation of IP-based mobility management schemes is based on simulation [20-23]. However, scenarios used for simulations vary greatly. This variation makes the comparison of IP-based handover protocols is hardly possible. Some presented schemes are based on multicast [23] where the MN sends an additional registration signaling traffic which causes additional overhead. Existing works of modeling mobile IP present studying the effect of handover on the performance without considering node mobility behavior.

This paper presents a performance evaluation analysis for original protocol for micro and macro handover cases. Then solves the problem of quantifying the degradation of quality of services (QoS) a mobile user perceives during macro and micro handover, and the signaling load costs associated with each case. From this point, a new scheme that develops F-HMIPv6 to avoid its drawbacks is proposed. Previous schemes based on F-HMIPv6 usually suffer from three major drawbacks: First, they don't consider the QoS of the traffic. Second, they focus only on the micro mobility level. Third, they don't exploit the information about the user mobility behavior in order to reduce handover effects.

In this paper, Macro Handover Mobility (MHM) scheme is proposed. It avoids these drawbacks by considering LBS that uses the available information about MN such as user mobility patterns and MN's velocity to predict handover and improve network's QoS. It also takes the traffic type into consideration since it presents a major factor in locating QoS for the user. This information is used efficiently to reduce handover latency and improve services. The performance of MHM is verified by analysis. The comparison between MHM and F-HMIPv6 shows a significant improvement in the performance of MHM in terms of packet delivery cost and location update cost under the variation of user

density and session-to-mobility ratio. The results also show an improvement of the hand-over latency in the proposed scheme over another scheme that is based on multicast.

The rest of this paper is organized as follows; the proposed MHM scheme is presented in Section 2. The analytic models are shown in Section 3. Section 4, presents the numerical results. Finally, the concluding remarks are given in Section 5.

2. The Architecture of the Proposed MHM Scheme

The proposed MHM scheme has the advantages of low latency and fast handover. In real life, most people usually follow a finite number of paths. For example, people leave their homes in the morning heading to work at a specific time and return home in the afternoon. The same applies to mobile users. According to this observation, the proposed scheme defines a number of mobility patterns based on user daily behavior. This information is used efficiently to reduce handover latency and improve services. The user may change his behavior at any moment. For example, if he would like to try something new such as traveling to another town in the weekend. In this case, he follows a new path which is not included in his known mobility profiles.

The proposed scheme adapts with such situations by following two procedures. First procedure involves updating the user's mobility profile to include this new path. Second procedure provides a seamless service to the user by using a buffering system to store MN's packets on macro mobility movement. Since the buffering time may affect on the performance of some traffic, the buffering system must be used properly and at the right time. MHM scheme uses buffering process for a limited number of MNs and for specific types of traffic that don't suffer from buffering delay. Then, MHM scheme keeps tracking MN's velocity and only uses the buffering system with mobility users that have high speed since they are exposed to many handovers. The proposed scheme also considers the traffic types. So it uses the buffering system exclusively with high reliability traffic. Examples of high reliability traffic are TCP traffic and bulk data transfer; where delays due to retransmissions are not important.

Fig. 2 shows the major components of the proposed MHM scheme. It consists of two main parts; prediction system in MN and buffering system in network components. Prediction system is presented as software package installed in MN's operating system. This package uses a learning algorithm to gather information about user behavior. This information is used to create user mobility profiles which can be used to predict the NAR in order to reduce handover latency. So the prediction system is mainly based on user mobility profiles. The second part is implemented in both hardware and software in the network. The software component keeps track of MN's velocity and traffic type. So, it would only invoke the buffering procedure with high speed MN that is dealing with high reliability traffic types. The buffering systems uses hardware components to represent buffers which store packets sent to the MN and can be retransmitted once the MN is registered in new AR.

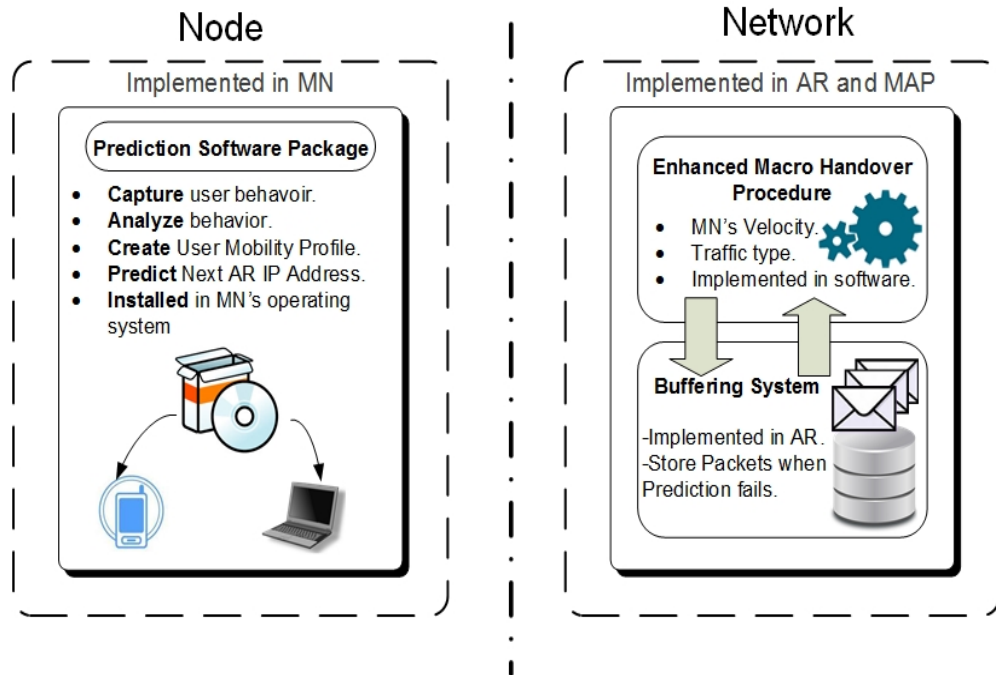


Fig. 2. MHM architecture.

MHM scheme has a structure that is similar to the structure of F-HMIPv6 networks, where each MN has a dedicated HA. Two-layer hierarchical of addressing is given in Fig. 3 Each MAP domain contains all the second layer nodes (ARs). The CN, the MN, and the HA are located in different domains. MHM scheme adds software package in MN to handle mobility profiles. This is used to predict NAR. Based on this information, the protocol updates its HA and all CNs with its new address before leaving its current network and entering a new one. It also considers executing enhanced procedure for high reliability traffic to high speed MN with unknown mobility pattern.

This enhanced procedure is designed to enable the MN to rapidly detect its movements and to obtain a new IP address with a NAR_N in MAP_N while being connected to NAR_P . Moreover, a bidirectional tunnel is setup between the MAP_P and MAP_N via the ARs to avoid packet drops. Then, the packets addressed to the MN are intercepted by the MAP_P and tunneled to the MAP_N . MHM is an effective integration that enables a MN to minimize exchanged signaling messages and reduce handover latency.

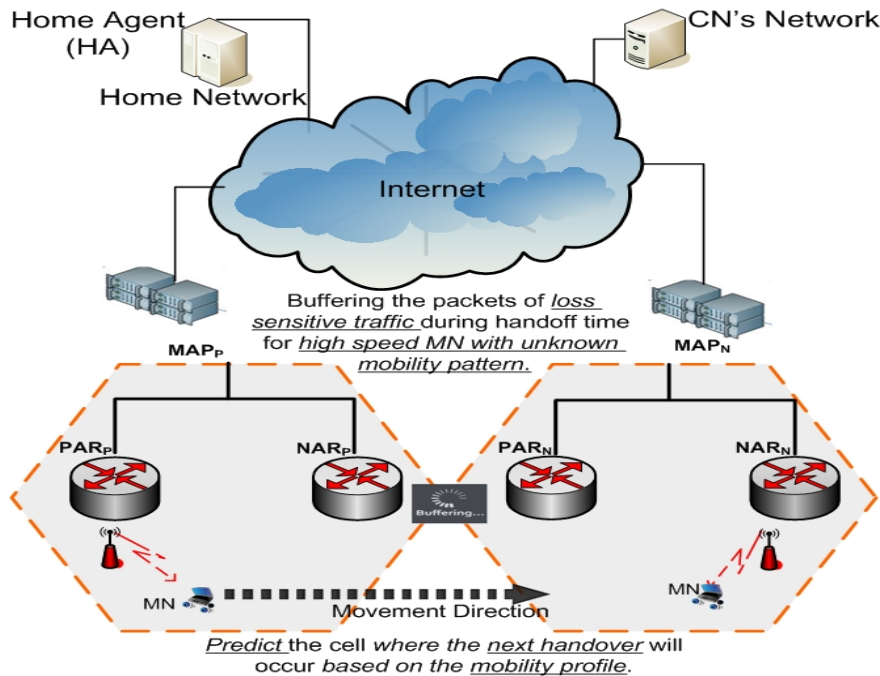


Fig. 3. MHM network model.

The main procedure of MHM works as follows: When L2 in MN indicates that there is available AR, it searches the stored mobility profile in MN for a path that contains the current AR's IP. If this search results in a number of matching paths, prediction system selects three paths that have highest weights and uses them to predict NAR's IP and its MAP. In this case, the prediction process becomes successful as it returns the paths containing MN's current point. Then, MN can register with NAR and send the LBU message to NARs. L2 starts the handover procedure and Layer 3 (L3) connection is lost. In the end, MN sends BU message to HA. All CNs will continue sending and receiving packets via NAR.

If there is no stored mobility profile for the current AR or in the case of false prediction; the prediction system is not activated, and then MN's velocity and the traffic type are checked. If MN's velocity exceeds a threshold value and MN deals with high reliability traffic type, the enhanced macro handover procedure will be invoked. Otherwise, the ordinary handover macro procedure will be executed since it is considered a sufficient solution for MN with low velocity or/and with loss insensitive traffic type.

The major steps followed in the proposed scheme are presented in the pseudo code in **Fig. 4**. This includes predicting the NAR's IP address and the registration with it before the handover time. If the system fails to do this prediction; high speed MN will request storage elements to buffer the high reliability packets during handover time. That is called Enhanced_Macro_Handover procedure. Otherwise, Ordinary_Macro_Handover procedure is implemented.

```

If (MN has mobility profile including the current point)
    Predict NAR's IP address and its MAP
    Perform registration with the predicted AR
Else
    Check MN's Velocity
    If (MN's velocity >  $v_{Th}$ )
        If (Traffic type is high reliability)
            Start Enhanced_Macro_Handover procedure
        Else
            Start Ordinary_Macro_Handover procedure
        End If
    Else
        Start Ordinary_Macro_Handover procedure
    End If
End If

```

Fig. 4. Pseudo code of the MHM main steps.

2.1 MHM Prediction System

MHM uses a prediction system that is implemented in MN to predict the NAR in order to reduce handover latency. The prediction is based on the information stored in user mobility profile. The system is presented as a software package that is installed on MN's operating system as a necessary step when the network is configured on the MN's device for the first time. This software works as a running service on the operating system that aims to collect information about the user and analyze this information to update user profile.

The prediction system works when the service faces L2 triggering situation in which L2 indicates that a NAR is available, or when it receives a better signal from NAR_N followed by the degradation of the PAR's signal. This type of events generated by L2 mechanisms, forces the prediction system to invoke AR's IP prediction algorithm to predict the NAR based on the existing mobility profile.

The program's main structure is represented by the pseudo code in **Fig. 5**, in which the main loop runs forever to present the running service that keeps track of the MN's different events such as L2 triggering or capturing user behavior.

```

do forever: // the main scheduler loop
    if event type == EndProgram:
        quit // break out of event loop
    else if event type == CTimeIntervalElapsed:
        //Capture user behavior every given amount of time (i.e. CTime=30 seconds)
        callCaptureBehavior procedure
    else if event type == L2Triggering:
        //Predict NAR and its MAP based on user profile
        call Registration procedure
    else if event type==AnalysisTrigger
        //Analyze user behavior every given amount of time (i.e. ATime=7 days)
        callAnalyzeBehavior procedure
    else handle unrecognized event
        // ignore or raise exception
end loop

```

Fig. 5. Pseudo code of main program.

The prediction system can be divided into two modules, the training module and the AR's IP prediction module:

i) The training module is shown in **Fig. 6**. The system trains itself to understand the user behavior. For example, most mobile users leave their homes in the morning heading to work using the same path every day. They probably would like to exploit the time they waste in transition between work and home. So they use their cell phones/laptops to accomplish work using network services that include dealing with different traffic types (i.e. FTP emails, voice Hifi, video playback and video conference).

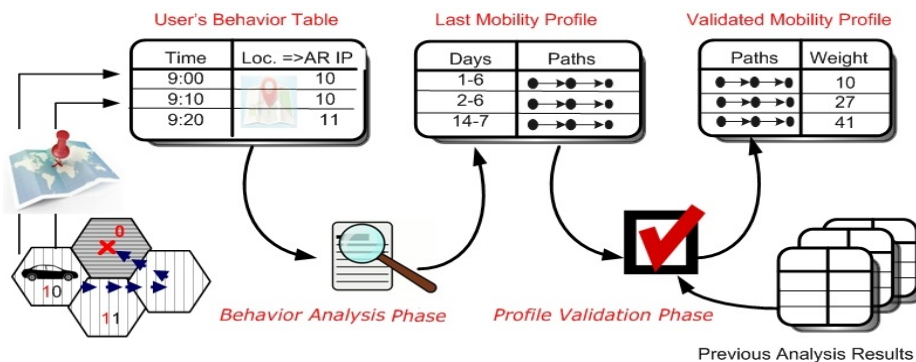


Fig. 6. Training procedure

The training system gathers information about the user which includes current AR's IP and MAP. The system captures this information every given amount of time called capture time. This information is stored in MN's memory to build the user behavior table. User behavior table contains records showing changing AR's IP and MAP along the user's day. The pseudo code of the "Capture Behavior" event handler is presented in **Fig. 7**.

```

Procedure CaptureBehavior
    Save new Record with AR, its MAP and Capture Time in User's behavior table
End Procedure

```

Fig. 7. Pseudo code of "Capture Behavior" procedure.

The second part in the training module is the analysis process. The system uses the gathered information and analyses it to configure mobility patterns for the user. The analysis process is executed after given amount of time called analysis time. The training module invokes analysis procedure which is shown in **Fig. 8**. In the analysis process, every captured event in the user's behavior table is analyzed. The output of the analysis procedure would be a mobility profile that shows a list of paths the user follows during the analysis time. For example, on the first day the user leaves home at 6:00 am, and goes to the work. In his way the user crosses the ARs [PAR_P , NAR_P , PAR_N , and NAR_N] at 6:30, 7:15, 8:00, and 9:00 am; respectively (**Fig. 3**). Then he arrives his work in NAR_N at 9:00 am, stays at work till 4:00 pm, and then returns to home passing ARs [NAR_N , PAR_N , NAR_P , and PAR_P].

Then, this path [PAR_P , NAR_P , PAR_N , NAR_N , PAR_N , NAR_P , and PAR_P] with its entry time is stored and linked to its day. This linked path presents a record in the generated user mobility profile that would contains a record for every day in the analysis period.

The mobility profile is the output of the analysis process. In order to have a result with high precision, the generated mobility profile must be validated with the previous mobility profile which was generated from the last analysis process.

```

Procedure AnalyzeBehavior
  //Extract days' information from behavior table
  Call ExtractDayList function
  Return (DayList)
  for i=0: (Length of DayList-1)
  Do
    CurrentDay= DayList[i]
    Call GetDayBehaviour (arguments: CurrentDay)
    Return (DayBehaviour)
    //Start creating user path in a given day
    DayMobilityProfile=null
    For j=0: (length of DayBehaviour -1)
    Do
      CurrentBehaviour= DayBehaviour[j]
      If (Current Behaviour's AR's IP is not the last AR IP in DayMobilityProfile)
        Add AR's IP with its Entry Time to DayMobilityProfile
      End if
    Next j
  Next i
  //Erase user behavior table data that are already analyzed
  Start garbage Collector
  //Validate the current analysis result with previous results
  Call ValidateAnlysisResult Function (Arguments: Last Mobility Profiles)
End Procedure

```

Fig. 8. Pseudo code of “Analyze Behavior” procedure.

Validation process involves comparing the results and shows what paths the user usually takes in his daily life. For example, the user usually takes the same path from home to work. So, this path is usually appears in user’s mobility profile. Validation emphasizes these paths and gives them high weights according to how much the user takes these paths. Validation process also takes notice if the user changes his daily behavior. For example, if the user changes his work place or moves to another house, a new path is detected. The program analyzes it and replaces the new path with the corresponding old one. This event considers a change in user behavior. The output of the validation system is the validated mobility profile and this is the profile in which the system uses to predict NAR’s IP.

- ii) The prediction system which is the AR’s IP prediction is presented in **Fig. 9**. In this procedure, the system inquires the mobility profile about the predicted NAR’s IP. This happens when L2 indicates that a NAR is available. In this case the system asks the mobility profile if the user has already experienced this AR’s IP at a time which is close to the current. Then, the mobility profile returns one or more matching paths. A selection algorithm is executed on the returned matching paths to choose three paths. The selecting algorithm takes the paths’ weight into consideration to select the chosen paths. The chosen paths return the predicted NAR’s IP so MN can start registering.

As expressed in **Fig. 10**, the handover prediction system includes three processes: the querying process which is presented in “FindPaths” function, the selection process

which is presented in “ApplySelectionAlgorithm” function, and the registration process which uses the returned predicted NAR’s IP to register MN with the NAR.

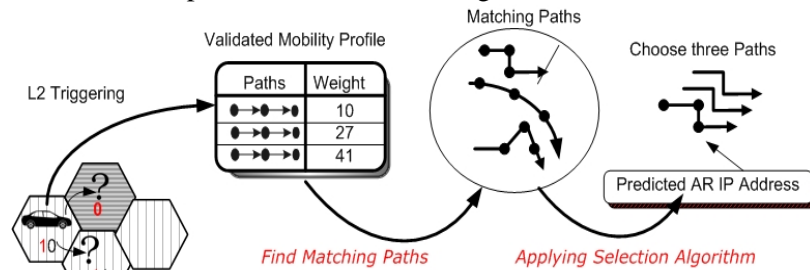


Fig. 9. Predicting mobility path procedures.

```

Procedure Registration
  //Search user profile for a path with the current AR and its MAP to expect the next AR
  Call FindPaths function (arguments: Current AR, Current MAP, Current_Time)
  Return MatchingPaths
  //Choose a path based on a selecting algorithm
  Call ApplySelectionAlgorithm function (arguments: MatchingPaths)
  Return (ChosenPaths)
  //Get next AR and its MAP from the chosen paths and start registering
  Start Registration procedure
End Procedure

```

Fig. 10. Pseudo code of “Registration” procedure.

2.2 MHM Buffering System

As it has been mentioned before, MHM uses the buffering system when prediction fails to predict NAR’s IP (i.e., the user tries a new path). Buffering time may affect on the performance of real-time traffic. Then, it is essentially to use and manage buffers efficiently in order to minimize overhead and to provide better QoS to different types of traffic. This is the main motive behind putting restrictions on invoking the buffering system. So, MHM scheme uses buffering process for macro mobility but for a limited number of MNs and for specific types of traffic. MHM extends the idea of fast handover on micro mobility movement to cover macro mobility level by adding a new macro procedure that tunnels between MAP_p and MAP_N through intermediate ARs. The steps of this enhanced procedure are represented in the pseudo code in **Fig. 11**.

The enhanced macro handover procedure starts by MN obtaining new LCoA and RCoA, then MAP_N receives LBU message to bind the MN’s LCoA with RCoA. MN sends FBU to MAP_p and HI message to MAP_N . The MAP_N verifies MN’s new RCoA and sends HI message to PAR_N which is verified by PAR_N . Then, PAR_N sends HACK message to MAP_N and MAP_N sends it to MAP_p . MAP_p sends the FBack message to MN and L2 starts the handover procedure. Then, L3 connection is lost. All packets destined to MN’s are stored in the PAR_p . When MN enters the new MAP domain, it sends FNA message to PAR_N and sends LBU to MAP_N . In case of successful delivery of the LBACK message to the MN, the PAR_N transfers the buffered packets to MN and MN sends BU message to HA and CN. The timing diagram is presented in **Fig. 12**. As noticed, the en-

hanced macro procedure uses the same control signals that are used during fast handover in micro mobility level. So, it does not add more complexity to the network model.

```

Procedure Enhanced_Macro_Handover
  MN Obtains LCoA (Local CoA).
  MN Obtains RCoA (regional CoA).
  MAPN receives LBU message to bind the MN's LCoA with RCoA.
  If (Binding is Successful)
    MN Sends FBU to MAPP.
    //Tunnel between MAPP and PARN is established.
    MAPP sends HI message to MAPN.
    MAPN verifies MN's new RCoA.
    MAPN sends HI message to PARN.
    PARN verifies the MN's new LCoA.
    PARN sends HACK message to MAPN.
    MAPN receives the HACK message and sends it to MAPP.
    //Tunnel between MAPN and MAPP is established to transfer the packets.
    MAPP sends the FBACK message to MN.
    Layer-2 starts the handover procedure.
    L3 connection will be lost
    While (Handover status is true)
      Packets destined to MN's current address.
      Packets are stored in buffer of the PARN.
    End While
    MN enters the new MAP domain.
    MN sends FNA message to the PARN.
    PARN transfers the buffered packets to the MN.
    If (buffered packets delivery is successful)
      MN sends the LBU message to MAPN.
    End if
    If (LBACK message delivery is successful)
      MN sends BU message to HA and all CN.
    End if
  End if
End Procedure

```

Fig. 11. Pseudo Code of “Enhanced_Macro_Handover” Procedure.

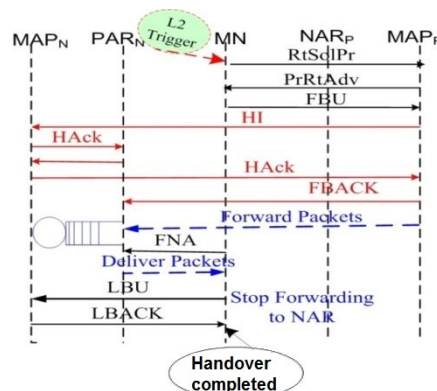


Fig. 12. Enhanced macro mobility location update in MHM.

Although the enhanced macro procedure increases the location update cost, it reduces the packet loss since that the time of macro handover is a long time compared to the mi-

cro handover. The gain of the enhanced macro procedure is much more than its additional cost. Moreover in order to reduce this additional cost, the enhanced macro procedure is invoked when necessary with a limited number of MNs and for specific types of traffic. If MN's velocity is under the threshold value or the traffic type it deals with doesn't have high reliability, the ordinary macro handover procedure is invoked. The MN obtains LCoA and RCoA. L2 starts the handover procedure and L3 connection is lost. When MN enters the new MAP domain, it sends the LBU message to MAP_N . In case of successful delivery of LBACK message to MN, the MN sends BU message to HA and all CN, and it sends and receives next packet via MAP_N .

3. Analytic Models

In IPv6-based wireless networks, QoS may be defined by packet loss, handover latency and signaling traffic overhead. Analysis of these metrics is very useful to assess the performance of mobility management protocols in IP-based mobile environments. An analytical framework for evaluating performance of the proposed MHM for different mobility models is presented in this section. The notation used is given in [Table 1](#).

3.1 Mobility Model

The mobile service areas (cells) are assumed as a hexagonal cellular architecture with equal size. Each cell is surrounded by rings of cells, except for cells in the outermost ring. Each domain is composed of k rings of the same size. The inmost cell labeled "0", the central cell. Cells labeled "1" constitute the first ring around cell "0", and so on. Each ring is labeled in accordance with the distance to the cell "0". [Fig. 13](#) shows an example of a MAP domain with two rings [\[24, 25\]](#).

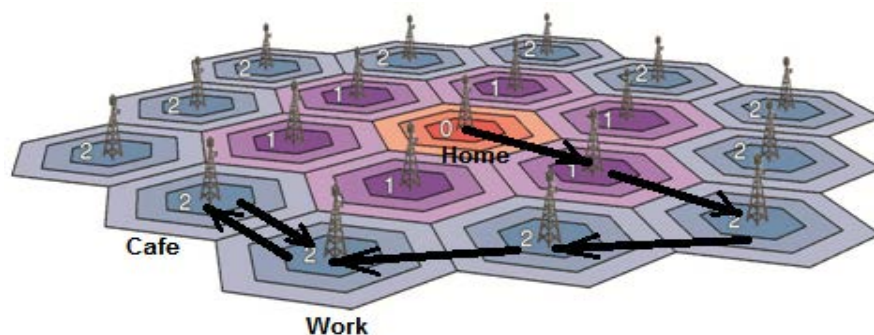


Fig. 13. Hexagonal cellular configurations in F-HMIPv6 architecture.

Table 1. List of notations

Symbol	Meaning
λ_m	The mean transmission time (/s).
λ_r	The mean cell residence time (/s).
σ	The user density in a cell (the average number of mobile users per square meter (/m ²)).
σ_r	The deviation of the velocity in city.
μ_{AR}	MN Movement (border crossing) rate out of an AR (the average number of crossings of the boundary of an AR per unit of time (/s)).
μ_{MAP}	MN Movement (border crossing) rate out of a MAP.
μ_S	MN Movement (border crossing) rate in which MN still stays within a MAP.
A_{AR}	The area of a cell domain (m ²).
A_{MAP}	The area of a MAP domain (m ²).
C_{BU}	The signaling cost function for total binding update
$C_{Buffered}$	The cost of transferring data packets from CN to MN by transiting to PAR and forwarding to NAR via the established tunnel.
C_{Data}	The cost of transferring data packets from CN to MN when the handovers fail.
C_{Known}	The signaling cost function for macro-mobility location update for known mobility pattern.
C_{Loss}	The packet loss cost.
C_{Macro}	The signaling cost function for macro-mobility location update.
C_{Macro_En}	The signaling cost function for enhanced macro location update procedure.
C_{Macro_Ord}	The signaling cost function for ordinary macro location update procedure.
C_{Micro}	The signaling cost functions for micro handover location update.
C_{PD}	The packet delivery cost
C_{T_L2}	The cost of elapsed time between L2 handover trigger and the establishment of a new link
C_{Tunnel}	The packet tunneling cost.
C_{Unknow}	The signaling cost function for macro-mobility location update for unknown mobility pattern.
$C_{X,Y}$	The transmission cost of a control packet between two nodes X and Y.
k	Number of the ARs within an MAP.
N_{CN}	Number of the CNs.
P_{L2}	The probability of anticipated handover signaling success.
P_{MAP}	The probability for an MN to perform an inter-domain location update.
PC_{AR}	The processing cost at the AR.
PC_{CN}	The processing cost at the CN.
PC_{HA}	The processing cost at the HA.
PC_{MAP}	The processing cost at the MAP.
PC_{MN}	The processing cost at the MN.
R	The number of rings in an MAP.
s_c	The average size of control packets (bytes).
s_d	The average size of data packets (bytes).
S_{hc}	The binding update cost at the HA and at all CNs.
S_{L2_f}	The signaling cost for control messages if no real L3 handover occurs.
S_{L2_s}	The signaling cost for a successfully anticipated handover.
S_{rr}	The signaling cost due to return routability procedure.
SMR	Session to mobility ratio.
t_{BU}	Location update latency.
t_{HA}	The delay for performing BU procedure to the HA(s).
t_{IP}	The IP connectivity latency(s).

t_{L2}	The link switching or L2 handover latency(s).
t_{NR}	The time of reception of first packet at the new IP address(s).
t_p	Packet reception latency or handover latency.
t_{rr}	The delay due to return routability procedure(s).
t_{TL2}	The time from L2 source trigger epoch to establishment of a new link.
t_U	The location updates latency(s).
v	The average speed of an MN (m/s).
v_{mean}	The mean velocities of city.
V_{Th}	The velocity threshold after it considers high speed MN.
w_{mr}	The weight factor for fraction of cars on major roads.

In terms of user mobility model, there are two commonly used mobility models: fluid-flow mobility model and random-walk mobility model. The fluid-flow model is more suitable for MNs with high mobility and static speed/moving direction. On the other hand, the random-walk model is more appropriate for pedestrian movements where mobility is generally confined to limited geographical area such as residential and business buildings [26]. However in addition to these models, it is proved in [15] that Baumann model is appropriate for any type of MN movement. Then, this mobility model is considered in the analysis.

Baumann mobility model finds the border crossing rate for which the MN out of an AR and the border crossing rate out of MAP. Furthermore, it finds the border crossing rate for which the MN out of an AR and still stays in the same MAP. When the MN crosses a MAP border, it also crosses an AR border. According to the state transition diagram in Fig. 14, the state i ($i \geq 0$) is defined as the number of AR that the MN passes within a single access network. The state transition $\mu_{AR(i,i+1)}$ ($0 \leq i < k$) represents the rate of MN's movement from one AR to another. The transitions $\mu_{MAP(i,0)}$ ($1 \leq i \leq k$) represent the movement to an AR out of the MAP [15].

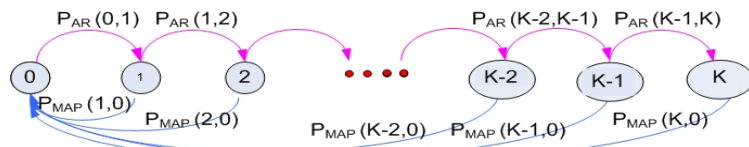


Fig. 14. State diagrams for of MN's movement.

If there are k sufficiently large ARs within a MAP, then the border crossing rate of MN may be defined as [15]. The movement rate out of an AR:

$$\mu_{AR} = \frac{2v}{\sqrt{\pi A_{AR}}} \tag{1}$$

The movement rate out of MAP:

$$\mu_{MAP} = \frac{\mu_{AR}}{\sqrt{k}} \tag{2}$$

The movement rate in which MN still within the same MAP:

$$\mu_S = \mu_{AR} - \mu_{MAP} = \mu_{AR} - \frac{\mu_{AR}}{\sqrt{k}} = \mu_{AR} \frac{\sqrt{k} - 1}{\sqrt{k}} \quad (3)$$

The mobility management procedure is used to implement the cost functions. These cost functions are used to analyze the performance of MHM. The implementation of cost functions consists of implementing location update cost, packet delivery cost and total cost.

3.2 MHM Cost Functions

Location update cost is represented by the number of control messages transferred during location update time. This cost can either appear in a wireless network or in a wired network. The transmission cost of a control packet between two nodes X and Y belonging to the wired part of a network can be expressed as $C_{X,Y} = \tau d_{X,Y}$, while the cost between two nodes in a wireless network can be represented as $C_{MN,AR} = \tau z$, where $d_{X,Y}$ is the hop distance between the two network elements X and Y, τ is the unit transmission cost over a wired link, and z is the weighting factor of the wireless link. Thus, the transmission cost in a wireless link is generally larger than the transmission cost in a wired link [27].

Depending on the type of movement and the mobility management protocol, two kinds of binding updates can be performed: micro handover (local) and macro handover (global). The former is the movement within a MAP administrative domain, while the latter implies movements between domains. The location update procedures are carried out for micro management and macro management. The following assumptions are used; the distance between PAR and MAP is equal to the distance between NAR and MAP, and the link layer information (L2 trigger) is used either to predict or rapidly respond to handover events.

3.2.1 Location Update Signaling Cost

Signaling cost function for micro handover location update C_{Micro} is expressed as follows [15]:

$$C_{Micro} = P_{L2} S_{L2_s} + (1 - P_{L2}) S_{L2_f} + S_h \quad (4)$$

The expression of S_{L2_s} presents the cost for a successfully anticipated handover and can be computed as:

$$S_{L2_s} = 4C_{MN,MAP} + 3C_{MAP,NAR} + 2C_{MN,NAR} + 3PC_{MAP} + 2PC_{AR} \quad (5)$$

and S_{L2_f} is expressed as follows:

$$S_{L2_f} = 3C_{MN,MAP} + PC_{AR} + 2(C_{MAP,NAR} + PC_{MAP}) \quad (6)$$

and S_h is introduced for convenient short form:

$$S_h = P_{L2}[2(C_{MN,NAR} + C_{NAR,MAP}) + PC_{AR} + PC_{MAP}] \\ + (1 - P_{L2})[2(2C_{MN,AR} + PC_{AR} + C_{MN,MAP}) + PC_{MAP}] \quad (7)$$

To drive the macro mobility location update cost, the probability P_{L2} of a successful handover signaling anticipation is assumed to be as large as possible. It reaches 1 when L2 successfully generates handover trigger. In case of successful handover signaling an-

icipation (i.e. $P_{L2}=1$), MHM scheme starts invoking the prediction system which either returns a known mobility pattern or unknown mobility pattern.

When the prediction system manages to successfully return a known mobility pattern and predict NAR's IP and its MAP, the location update cost starts as soon as L2 generates handover trigger. So, the location update cost is considered to be the maximum cost between the registration cost and the cost of reestablishing new link. Then, the location update cost for known mobility pattern C_{Known} can be represented as follows:

$$C_{Known} = PC_{MN} + \text{Max}(C_{Macro_Ord}, C_{T_L2}) \quad (8)$$

where C_{Macro_Ord} can be expressed as:

$$C_{Macro_Ord} = 4C_{MN,AR} + 2PC_{AR} + S_{hc} \quad (9)$$

The expression of S_{hc} can be expressed as:

$$S_{hc} = 2(C_{MN,HA} + N_{CN}C_{MN,CN}) + PC_{HA} + N_{CN}PC_{CN} + S_{tr} \quad (10)$$

while S_{tr} is the signaling cost due to return routability procedure; it can be computed as follows:

$$S_{tr} = 2(C_{MN,HA} + N_{CN}C_{HA,CN} + N_{CN}C_{MN,CN} + PC_{HA} + N_{CN}PC_{CN}) \quad (11)$$

and C_{T_L2} is the cost of elapsed time between L2 handover trigger and the establishment of a new link.

As mentioned earlier, an additional processing time in the MN is added for storing or retrieving mobility profile PC_{MN} , which is necessary for the prediction system to predict NAR's IP. PC_{MN} is measured as a small value that is not compared to the location update cost. On the other hand, it helps to reduce the packet loss during L3 handover. In practical experiments, PC_{MN} ranges between 30 to 50 milliseconds, as it considers as a simple process to retrieve stored data [28]. For unknown mobility profile, the MHM scheme either invokes the enhanced macro procedure or the ordinary macro procedure.

The cost of invoking the enhanced macro procedure can be expressed as

$$C_{Macro_En} = 2C_{MAP_p,MAP_N} + 4C_{MN,NAR_N} + 3C_{MAP_N,NAR_N} + 2C_{MN,NAR_N} + 6PC_{MAP} + 3PC_{AR} + 2(C_{MN,NAR_N} + C_{NAR_N,MAP_N}) + S_{hc} \quad (12)$$

As noticed, there is an additional cost for creating a tunnel between MAP_p and MAP_N via NAR_p and PAR_N . In other situations, MHM scheme may invoke the ordinary macro procedure. The cost of invoking such procedure is the cost of the registration with a new MAP which is expressed in (13). The total cost due to the macro mobility location update for unknown mobility pattern can be expressed in (16). The equation represents the total cost whether the enhanced macro procedure was invoked or the ordinary macro procedure was invoked.

$$C_{Unkown}(i) = I_i C_{Macro_Ord} + \bar{I}_i C_{Macro_En} \quad (13)$$

$$I_i = \begin{cases} 1, & \text{if ordinary macro handoff scheme occurs at time } i \\ 0, & \text{otherwise.} \end{cases} \quad (14)$$

$$\bar{I}_i = \begin{cases} 1, & \text{if enhanced macro handoff scheme occurs at time } i \\ 0, & \text{otherwise.} \end{cases} \quad (15)$$

The location update cost for both procedures of macro handover at time i :

$$C_{\text{Unknown}} = C_{\text{Macro_Ord}} \times (1 - \Pr(v > V_{\text{Th}} \& \text{traffic is high reliability})) + C_{\text{Macro_En}} \times \Pr(v > V_{\text{Th}} \& \text{traffic is high reliability}) \quad (16)$$

where

$$\Pr(v > V_{\text{Th}} \& \text{traffic is high reliability}) = \Pr(v > V_{\text{Th}}) \times \Pr(\text{traffic is high reliability}) \quad (17)$$

$$\Pr(v > V_{\text{Th}}) = \int_{V_{\text{Th}}}^{\infty} f_v(\sigma_r, v_{\text{mean}}, v) dv \quad (18)$$

with velocity density function [25]:

$$f_v(\sigma_r, v_{\text{mean}}, v) = \left\{ \frac{1}{1 + w_{\text{nr}}} \left[\frac{v}{\sigma_r^2} e^{-\frac{v^2 + v_{\text{mean}}^2}{2\sigma_r^2}} I_0 \left(\frac{v \cdot v_{\text{mean}}}{\sigma_r^2} \right) \right] \right\} \quad (19)$$

The total cost of macro handover mobility in both cases of known and unknown mobility pattern can be expressed as follows:

$$C_{\text{Macro}} = (1 - \Pr(\text{NAR successfully predicted})) C_{\text{Unknown}} + \Pr(\text{NAR successfully predicted}) C_{\text{Known}} \quad (20)$$

where $\Pr(\text{NAR successfully predicted})$ depends on how well the prediction system can predict NAR's IP and its MAP, and it's mainly depends on user's behavior. For most mobility users with a fixed daily routine, the probability of successful prediction is as large as possible. On the other hand, in case of users continually change daily paths, the prediction fails and MHM invokes ordinary or enhanced procedure which leads to a lower total cost.

Total binding update signaling cost with the random walk mobility model [15]:

$$C_{\text{BU}} = \frac{P_{\text{MAP}} \times C_{\text{Macro}} + (1 - P_{\text{MAP}}) \times C_{\text{Micro}}}{\lambda_r} \quad (21)$$

Total location update cost with the fluid-flow mobility model [15]:

$$C_{\text{BU}} = \frac{\mu_{\text{MAP}} \times C_{\text{Macro}}}{\sigma \times A_{\text{MAP}}} + \frac{(R \times \mu_{\text{AR}} - \mu_{\text{MAP}}) \times C_{\text{Micro}}}{\sigma \times A_{\text{MAP}}} \quad (22)$$

The total binding update signaling cost per MN for the Baumann mobility model is expressed as follows:

$$C_{\text{BU}} = \frac{1}{\lambda_m} (\mu_{\text{MAP}} \times C_{\text{Macro}} + \mu_{\text{AR}} \times C_{\text{Micro}}) = \frac{1}{\text{SMR} \sqrt{k}} [C_{\text{Macro}} + (\sqrt{k} - 1) C_{\text{Micro}}] \quad (23)$$

3.2.2 Packet Delivery Cost

The packet delivery cost is defined as the linear combination of packet tunneling cost (C_{Tunnel}) and packet loss cost (C_{Loss}) during handover latency. Let α and β be weighting factors (where $\alpha + \beta = 1$), which emphasize tunneling effect and dropping effect. Then, the packet delivery cost is computed as follows:

$$C_{\text{PD}} = \alpha C_{\text{Tunnel}} + \beta C_{\text{Loss}} \quad (24)$$

The handover latency is divided into three components: link switching or L2 handover

latency (t_{L2}), IP connectivity latency (t_{IP}) and location update latency (t_{BU}). IP connectivity latency reflects how quickly an MN can send IP packets after L2 handover, while location update latency is the latency of forwarding IP packets to MN's new IP address. The time from the starting point of L2 handover to when an MN first receives IP packets for the first time after link switching refers to packet reception latency (t_p) or handover latency.

Fig. 15 presents the timing diagram associated to macro mobility of MHM for known mobility pattern. The elapsed time between L2 handover trigger and the establishment of a new link is used to make a connection to the NAR and its MAP. So packet loss cost can be expressed as:

$$C_{Loss} = \lambda_m C_{Data} (\max(t_{TL2} + t_{L2}), (t_{TL2} + t_{IP} + t_U)) \tag{25}$$

where

$$t_U = t_{HA} + t_{rr} + t_{CN} + t_{NR} \tag{26}$$

and

$$C_{Data} = \eta(C_{CN,MAP} + C_{MAP,PAR} + C_{PAR,MN} + PC_{MAP}) \tag{27}$$

where

$$\eta = s_d/s_c. \tag{28}$$

This represents the ratio between cost of transferring data packet and the cost of transferring control. For known mobility pattern, there may be no buffering. So, C_{Tunnel} will be equal to zero.

MHM also supports buffering and forwarding packets during macro handover since it chooses either to invoke the enhanced macro procedure or to invoke the ordinary macro procedure. MHM uses the enhanced macro procedure to reduce packet loss during the delay time consumed in link switching, IP connectivity latency and macro location update.

Fig. 16 presents the timing diagram associated with enhanced macro handover. It shows that there is a delay before an MN begins to receive packets directly through the NAR and update binding in HA and all active CN.

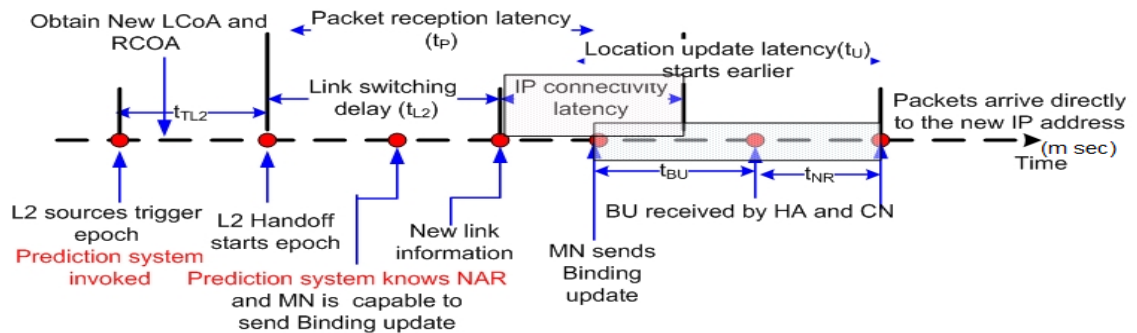


Fig. 15. Handover delay timeline of known handover in MHM

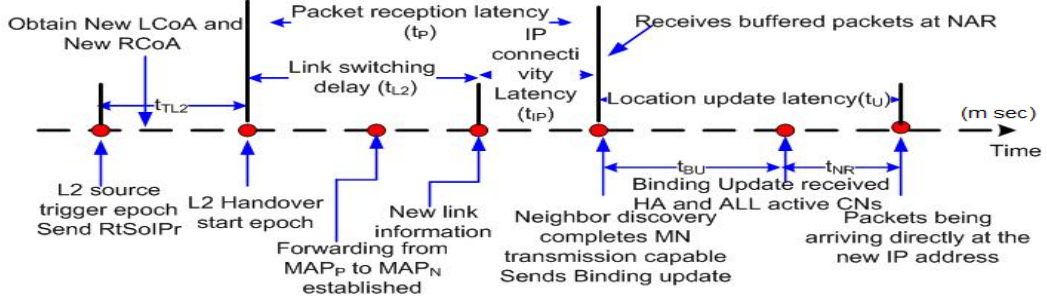


Fig. 16. Handover delay timeline of enhanced macro handover in MHM.

The packet delivery cost for macro mobility can be computed through (24), where packet loss cost C_{Loss} is:

$$C_{Loss} = \lambda_m C_{Data}(t_{L2}) \quad (29)$$

As expected the packet loss cost C_{Loss} for the enhanced macro procedure is less than the cost of ordinary macro procedure. However, there is additional cost for buffering the packets sent during macro handover as in:

$$C_{Tunnel} = \lambda_m C_{Buffered}(t_{L2} + t_{IP} + t_U) \quad (30)$$

where

$$C_{Buffered} = \eta(C_{CN,MAP} + C_{MAP,PAR} + C_{MAP,MAP} + C_{MAP,NAR} + C_{NAR,MN}) \quad (31)$$

The routing cost in MAP is proportional to the logarithm of the number of ARs and user's density in the MAP domain.

3.2.3 Total Cost

Total cost is defined as the sum of location update cost and packet delivery cost, and it is expressed as [15]:

$$C_{Total} = C_{BU} + C_{PD} \quad (32)$$

4. Simulation Results for Prediction

In this section the simulation result for prediction system is introduced. We examined the typical behavior of a mobile user by supposing several scenarios for a certain user. Software program is built to capture MN behavior. Then, the program was tested to ensure the capability of the learning process by testing it with new scenarios that either different or similar to known mobility patterns of the learned scenarios. Software package is implemented for android systems. Android is a widely anticipated open source operating system for mobile devices. MHM prediction system is developed using Java software development kit with LBS system application.

To better understand how a MN's mobility pattern is created, suppose the scenario shown by arrows in Fig. 13. The mobile user's residence is located in cell '0', while its place of work is located in cell '2'. It is considered that, the user leaves home at 08:00 am each morning. During its trip from home to work, the user crosses cells labeled '1', '2', '2'

and finally arrives another cell labeled '2'. The user has a break every day at 12:00 pm at the cafe located in cell '2'. At about 06:00 pm, the user leaves work in the direction of its residence passing through the same cells as in the morning but in the opposite order.

It is assumed that each day is divided into periods that represent the capture times. Capture time is assumed to be 30 min. To decrease the overhead resulting from saving the different paths during the day, 8 hours are ignored that represent the sleeping hours. Then, the remaining 16 hours are divided into 32 capture points. The analysis time is assumed one week to configure mobility patterns from the capture points. Table 2 shows the points of success or fails of the stored paths during the first week. Only 16 points out of the 32 points are tabulated in order to compress the results. Predicting the correct path is represented by (\checkmark), whereas the faults are represented by (x). The faults are distributed according to the random positions that the MN moves during each day. The result of each row represents the average faults per point and the result of each column represents the average faults per day. Then, the average faults during the first week are calculated. The last column represents the average faults during the second week.

It is shown that the total average faults in the first week is 17.86%, whereas this value is decreased to 16.75% in the second week since the program is acquired more learning and then it updated the stored paths according to the movement of the MN during the first week. This value is changed by $\pm 1\%$ during the consequence weeks. From **Table 2**, the average value of two weeks 16.96% is considered in our analysis as the value of the percentage of faults during the prediction system. So this value can be used in (20) as the value for probability of unknown pattern that is required in order to evaluate the total macro cost.

Table 2. Points of success and fails

Points /Day	First Week							Avg. Faults /Point (First week)	Avg. Faults /Point (2 weeks)
	Saturday	Sunday	Monday	Tuesday	Wednesday	Thursday	Friday		
1	X	\checkmark	\checkmark	\checkmark	X	\checkmark	\checkmark	28.57%	23.81%
2	X	X	\checkmark	\checkmark	\checkmark	\checkmark	\checkmark	28.57%	28.57%
3	X	X	\checkmark	\checkmark	\checkmark	\checkmark	\checkmark	28.57%	33.33%
4	\checkmark	\checkmark	X	\checkmark	\checkmark	\checkmark	\checkmark	14.29%	9.52%
5	\checkmark	\checkmark	X	\checkmark	\checkmark	\checkmark	\checkmark	14.29%	14.29%
6	\checkmark	\checkmark	\checkmark	\checkmark	\checkmark	\checkmark	X	14.29%	19.05%
7	\checkmark	\checkmark	\checkmark	\checkmark	X	\checkmark	X	28.57%	23.81%
8	\checkmark	\checkmark	\checkmark	\checkmark	\checkmark	\checkmark	X	14.29%	9.52%
9	\checkmark	\checkmark	X	X	X	\checkmark	\checkmark	42.86%	38.10%
10	\checkmark	\checkmark	X	\checkmark	\checkmark	\checkmark	\checkmark	14.29%	14.29%
11	\checkmark	\checkmark	\checkmark	\checkmark	\checkmark	\checkmark	\checkmark	0%	4.76%
12	\checkmark	\checkmark	\checkmark	\checkmark	\checkmark	\checkmark	\checkmark	0%	9.52%
13	\checkmark	X	\checkmark	\checkmark	\checkmark	\checkmark	\checkmark	14.29%	9.52%
14	\checkmark	X	\checkmark	\checkmark	\checkmark	\checkmark	\checkmark	14.29%	9.52%
15	\checkmark	X	\checkmark	\checkmark	\checkmark	X	\checkmark	28.57%	23.81%

16	√	√	√	√	√	√	√	0%	0%
Avg. Faults/Day	18.75%	31.25%	25%	6.25%	18.75%	6.25%	18.75%	17.86%	16.96%

5. Numerical Results

This section presents various analyses results based on the MHM's analytical model. The parameter values for the analysis were referenced from [9]. The experiments performed to evaluate the value of PC_{MN} and the estimated value of processing time in MN was in range 30-50 milliseconds [29]. **Table 3** presents the values of the system's parameters. The goal of MHM scheme is to minimize both packet loss and location update cost. It exploits the stored information in MN mobility profile in order to guarantee QoS requirements of various applications. **Table 4** presents different requirements for some IP services.

The analysis results involve studying the MHM's impact on the different types of cost functions. There are various parameters that should be considered such as user's velocity, traffic types, packet arrival rate, user density and session-to-mobility ratio (SMR) since they have a considerable impact on different types of cost. For example, location update cost depends on the user velocity; the user density influences packet delivery cost, while total cost is affected by SMR.

Table 3. The system parameters' values.

System Parameter	Value
N_{CN}	2
P_{L2}	0.8:1
R	500 m
S_c	200 bytes
S_d	96 bytes
α	0.2
β	0.8
k	10
σ	0.002
PC_{AR}	8
PC_{HA}	24
PC_{CN}	4
PC_{MAP}	12
PC_{MN}	50
w_{mr}	0.5
v_{mean}	60 Km/s
σ_r	20km/s
V_{Th}	100

Table 4. Characteristics and requirements for IP services

Information Type	Loss rate	Delay (ms)
Content data (file transfer e.g., E-mail).	-5	100
Content data (Remote process control).	-6	300
Hifi sound (Voice, recorded).	-7	100
Telephone (Voice, interactive).	-3	50
Video playback (Video, recorded).	-6	300
Videophone (Video, interactive).	-8	150
Video conference (Video, interactive)	-9	30

5.1 Location Update Cost

Fig. 17 depicts location update cost variation when the MN's mean velocity is changed with different values of V_{Th} in the case of Baumann mobility model. As expected, the MN performs fewer movements as the average residence time of the MN increases. Therefore, the location update cost is inversely proportional to the average residence time. It is shown that, the location update cost increases as the average velocity increases since the MN with a higher average velocity has a higher domain crossing rate. As expected when the velocity threshold decreases, the enhanced procedure tends to be executed with a higher location update cost. A known mobility pattern realizes minimum locations update cost.

5.2 Packet Loss Cost

In **Fig. 18**, the impact of some traffic types (shown in **Table 4**) on the packet loss cost is investigated. In the proposed case study, the prediction system is supposed to always fail and MN's velocity will always exceeds V_{Th} . So, the packet loss cost is depicted as a function of traffic type. **Fig. 18** shows the packet loss costs for a high reliability traffic type (video play pack) and two interactive applications (videophone and video conference). As the user exceeds the threshold velocity for the high reliability traffic type with unknown mobility pattern, the proposed scheme tends to be executed more frequently. So, the packet loss cost is reduced. For the other interactive data types, adding delay time for buffering process is unacceptable. Then, the proposed scheme does not have a considerable impact on the packet loss cost since it is not invoked for these traffic types.

For high reliability traffic types, the impact of packet arrival rate on the packet loss cost is shown in **Fig. 19**. It shows that the packet loss cost increases proportionally with the packet arrival rate λ_m . So, the proposed scheme becomes more efficient when λ_m increases as it is invoked to reduce the packet loss cost for MN with high speed.

It is also observed from the figure that when the arrival rate's value reaches 5 packets/s, the loss cost for all traffic types in the case of known mobility pattern is around 20, which is suitable for almost all applications. However, using the proposed scheme would make the cost value ranges from 40 to 65. This result depends on V_{Th} which controls the invoking of the buffering system.

5.3 Packet Delivery Cost

In general, the location update cost is affected by the user mobility and not by the user population. On the other hand, the packet delivery cost depends on user density as the MAP needs to determine whether the destination MN belongs to the mapping table or not. The cost of this lookup procedure is generally proportional to the number of MNs in the MAP domain. Therefore, the packet delivery cost increases as the number of MNs in the MAP domain increases. Fig. 20 shows the packet delivery cost as a function of the MN density (ρ). The results show that, the packet delivery cost increases linearly as the number of MNs increases. For a known mobility profile, the MHM achieves the least packet delivery cost.

5.4 Total Cost

Total cost combines the location update cost and the packet delivery cost. Fig. 21 and Fig. 22 show the total cost as a function of SMR in the Baumann model at the two cases $SMR \leq 1$ and $SMR > 1$; respectively. The SMR is equal to λ_m / μ_{AR} , which is the session arrival rate divided by the cell crossing rate.

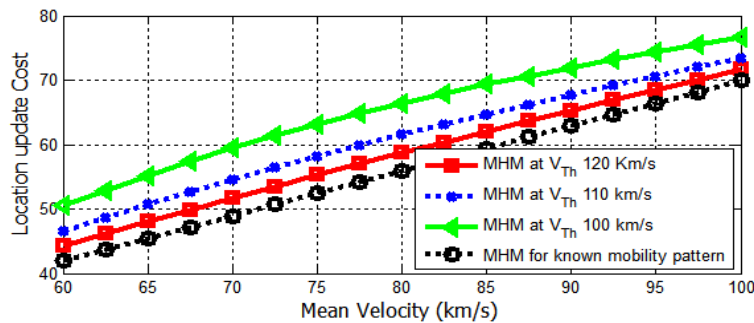


Fig. 17. Location update cost as a function of mean velocity.

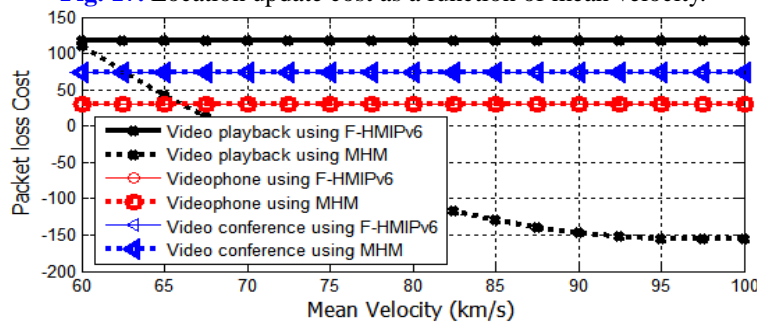


Fig. 18. Packet loss cost as a function of mean velocity.

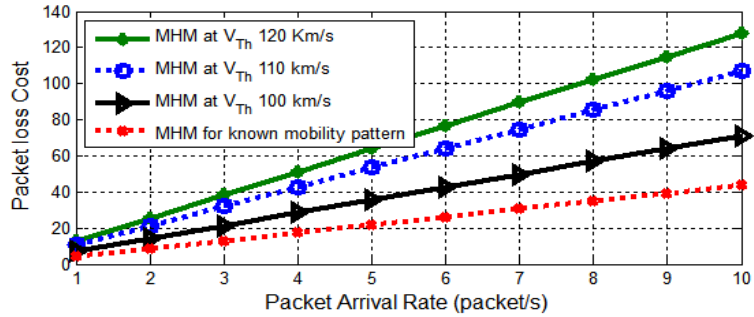


Fig. 19. Packet loss cost as a function of packet arrival rate

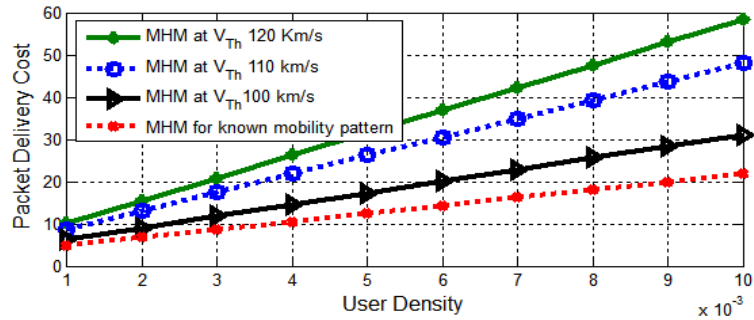


Fig. 20. Packet delivery cost as a function of user density.

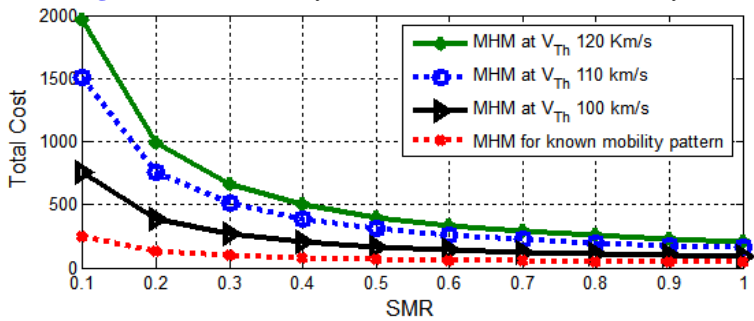


Fig. 21. Total cost as a function of SMR (SMR<1).

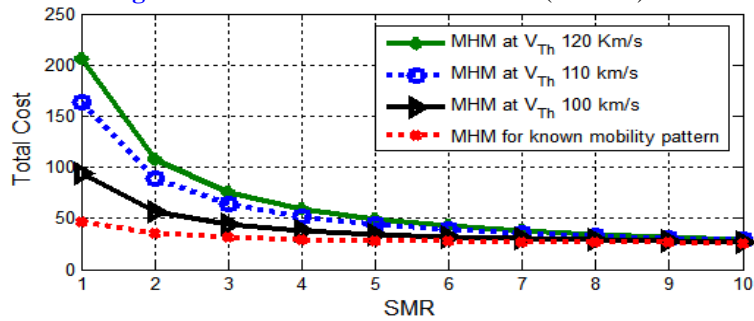


Fig. 22. Total cost as a function of SMR ($1 < SMR \leq 10$).

In the case of $SMR \leq 1$, i.e. $\lambda_m \leq \mu_{AR}$, the location update cost is more dominant in the total cost than packet delivery cost since the mobility rate is highly effective in the total cost than the transmission rate. However, at $SMR > 1$, the transmission rate is larger than mobility rate and then, binding update is less performed and signaling overhead is decreased. So the impact of the location update cost is reduced, while the packet delivery becomes more effective. Even though MHM increases the location update cost, it highly reduces the packed delivery cost which results in achieving less total cost.

5.5 Comparison between MHM and F-HMIPv6

This section presents a comparison between MHM and F-HMIPv6. The results for location update cost, packet loss cost, packet delivery cost, and total cost are investigated for both MHM and F-HMIPv6. The impact of user mobility on the location update cost is investigated. Fig. 23 shows the location update cost as a function of mean velocity for both MHM and F-HMIPv6 with Baumann model. As expected, MHM with known mobility pattern achieves the smallest cost as it starts the registration process as earlier as possible. MHM with unknown mobility pattern depends on the velocity and traffic type. In this figure, high reliability traffic type is assumed in order to isolate the impact of velocity on location update cost. So, the impact of mean velocity can be well investigated. The figure shows that the cost for both MHM for unknown mobility pattern and F-HMIPv6 are the same for velocity value that is lower than the threshold. When the velocity goes higher than the threshold value, the buffering process of MHM is invoked and the location update cost increases.

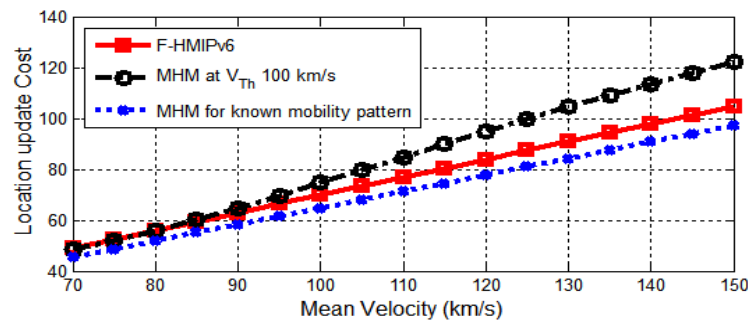


Fig. 23. Location update cost as a function of mean velocity.

In general, packet loss cost can be investigated independently on user mobility model since that the packet loss depends on the loss during the macro handover. Fig. 24 shows the packet loss cost variations for F-HMIPv6 and MHM. As the user exceeds the threshold velocity with high reliability traffic types, MHM with unknown mobility pattern tends to execute the enhanced scheme more often. So, it achieves smaller packet loss cost than F-HMIPv6. As expected, MHM with known mobility achieves the smallest loss cost. The decrease in the packet loss in the case of MHM reaches about 65% with respect to F-HMIPv6.

Fig. 25 shows the packet delivery cost as the MN density changes. The packet delivery cost increases as the number of MNs increases. It is shown that, F-HMIPv6 achieves the

highest packet delivery cost, while MHM with unknown mobility pattern achieves a lower packet delivery cost. The reason is that, the F-HMIPv6 behavior depends on buffering at micro level and this increase the packet delivery cost however the buffering process in MHM with unknown mobility pattern depends on MN velocity. It is also shown that, MHM with known mobility pattern achieves delivery cost of 47% less than F-HMIPv6.

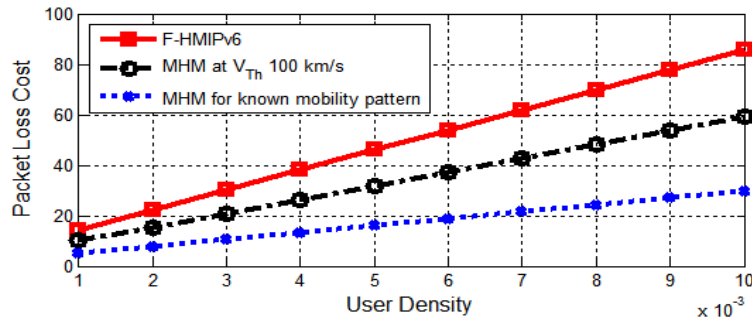


Fig. 24. Packet loss cost as a function of user density.

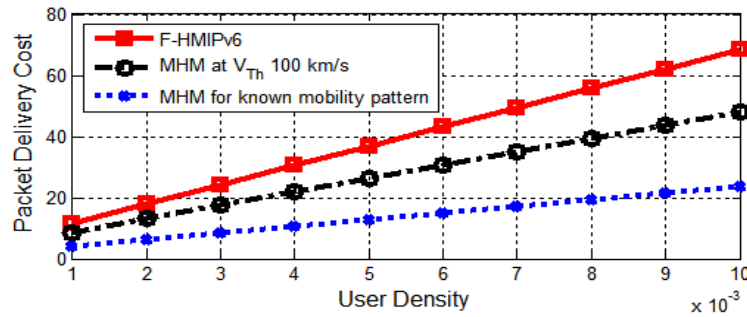


Fig. 25. Packet delivery cost as a function of user density.

Fig. 26 and Fig. 27 show the total cost as a function of SMR for MHM with known and unknown mobility patterns and F-HMIPv6. All the results are investigated for both SMR>1 and SMR≤1. In the Bumman model, SMR is equal to λ_m / μ_{AR} . As shown before, at SMR≤1 the impact of location update cost is increased while packet delivery cost becomes less effective in the total cost. It is shown that MHM with known mobility pattern achieves the least total cost, while MHM with unknown mobility pattern depends on the velocity and traffic type. In these figures, high reliability traffic type is assumed and the velocity exceeds the threshold in order to show the impact of velocity. In this case, the buffering process of MHM is invoked and the location update cost increases that increases the total cost than F-HMIPv6.

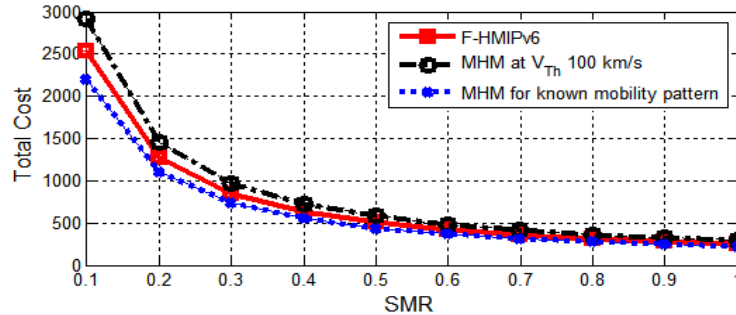


Fig. 26. Total cost at $SMR \leq 1$ (Baumann model).

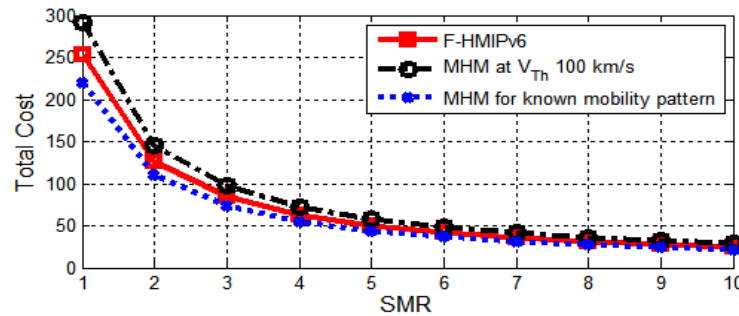


Fig. 27. Total cost at $1 < SMR \leq 10$ (Baumann model).

5.6 Handover Latency

In this section, the handover latency comparison between F-HMIPv6, MHM for known mobility pattern and for unknown mobility pattern at $V_{Th}=100$, and another scheme that is based on multicast [23] is summarized in Table 5.

Table 5. Macro and micro-mobility handover latency

Scheme	Macro-mobility handover time	Micro-mobility handover time
	(ms)	(ms)
FHMIPv6	2.39	0.20
MHM for known mobility pattern	0.51	0.13
MHM at $V_{Th}=100$ for unknown mobility pattern	2.39	0.20
Scheme based on multicast [23]	1.24	1.96

It is shown that, MHM for known mobility pattern achieves the least macro-mobility and micro-mobility handover latencies. These latencies are equal to 0.51 and 0.13; respectively which means that it takes short time for the transmission of registration because the prediction process becomes successful as it returns the paths containing MN's current point. Then, MN can register with NAR as early as possible. Another situation is analyzed as the prediction system fails with MN's mean velocity is assumed as in Table 3. So MN's velocity doesn't exceed the threshold value. In this case, macro-mobility and micro-mobility handover latencies are identical with F-HMIPv6. In addition, the scheme based on multicast [23] has smaller values than F-HMIPv6. However, there is an increas-

ing in micro-mobility handover latency due to an increase in the number of registration based on multicast procedure for all neighbors AR. This increasing exceeds macro-mobility handover latency, which is not acceptable especially for high reliability traffic.

6. Conclusion

The paper proposed a new scheme for smooth handover over F-HMIPv6 networks in the macro mobility. The proposed architecture of MHM is based on a software package in each MN and a hardware part in the network side. Each package is responsible for capturing information about user behavior, and exploiting this information to create user mobility profiles. MHM extends the idea of fast handover on micro mobility movement to cover macro mobility level by adding a new macro procedure.

The performance of MHM and F-HMIPv6 are compared in terms of packet delivery cost and location update cost. The numerical results showed that MHM with known mobility profiles achieves the smallest cost as it starts the registration process as earlier as possible however; MHM with unknown mobility profiles depends on the velocity and traffic type. The results showed that the cost for both MHM and F-HMIPv6 are the same for velocity values that are lower than a threshold. When the velocity goes higher than the threshold value, the proposed scheme manages to reduce the packet loss for high reliability traffic types by buffering process that increases the location update cost. MHM reflects an optimized smooth handover better than F-HMIPv6 and achieves an improvement in the cost reaches about 40% in some situations. The proposed MHM has implications for communication, design, and pricing of mobile services. It provides insights for designers on how to realize smooth handovers required for multimedia services while guaranteeing the lowest cost as possible that is the demand for all customers of mobile services.

References

- [1] Y. Chon, E. Talipov, H. Shin, H., "SmartDC: Mobility Prediction-Based Adaptive Duty Cycling for Everyday Location Monitoring," *IEEE Transactions on Mobile Computing*, vol.13, no. 3, pp. 512-525, March 2014. [Article \(CrossRef Link\)](#)
- [2] Y. Lin, C. Huang-Fu, and N. Alrajeh, "Predicting human movement based on Telecom's handover in mobile networks," *IEEE Transactions on Mobile Computing*, vol. 12, no. 6, pp. 1236-1241, June 2013. [Article \(CrossRef Link\)](#)
- [3] C. Anagnostopoulos, K. Kolomvatsos, and S. Hadjiefthymiade, "Efficient location based services for groups of mobile users," in *Proc. of IEEE 14th International Conference on Mobile Data Management (MDM)*, Italy, pp. 6-15, June 2013. [Article \(CrossRef Link\)](#)
- [4] D. Johnson, C. Perkins, and J. Arkko, "Mobility Support in IPv6," *Internet Soc., Reston, VA, IETF RFC 3775*, January 2004. [Article \(CrossRef Link\)](#)
- [5] W. Xiaonan, and Z. Shan, "Research on mobility handover for IPv6-based MANET," *Trans. Emerging Tel Tech*, vol. 25, pp. 679-691, 2014. [Article \(CrossRef Link\)](#)
- [6] R. Koodli, "Mobile IPv6 Fast Handovers," *Internet Soc., Reston, VA, IETF RFC 5568*, July 2009. [Article \(CrossRef Link\)](#)

- [7] H. Soliman, C. Castelluccia, K. ElMalki, and L. Bellier, "Hierarchical mobile IPv6 (HMIPv6) mobility management," *Internet Soc., Reston, VA, IETF RFC 5380*, October 2008.
[Article \(CrossRef Link\)](#)
- [8] D.K. Panwar, D.K. Lal, and I. Chaudhary, "Handover latency analysis of mobility management protocols in all-IP networks," in *Proc. of Advances in Computing, Control, & Telecommunication Technologies (ACT '09)*, pp. 390-394, December 2009.
[Article \(CrossRef Link\)](#)
- [9] H. Nashaat, R. Rizk and H. Mahdi, "A robust analytical model of mobile IP handover with multiple traffic profile," *International Journal of Wireless Information Network, Springer*, vol. 18, no. 4, pp. 210-223, 2011. [Article \(CrossRef Link\)](#)
- [10] H. Nashaat, R. Rizk, and H. Mahdi, "Performance analysis of streamed video over mobile IP based networks," in *Proc. of 9th IEEE/ACS International Conference on Computer Systems and Applications (AICCSA)*, Egypt, December 2011. [Article \(CrossRef Link\)](#)
- [11] N. Kara, "Mobility management approaches for mobile IP networks: performance comparison and use recommendations", *IEEE Transactions on Mobile Computing*, vol. 8 , no. 10, pp. 1312 – 1325, October 2009. [Article \(CrossRef Link\)](#)
- [12] J.-H. Lee, T. Ernst, and T.-M. Chung, "Cost analysis of IP mobility management protocols for consumer mobile devices," *IEEE Transactions on Consumer Electronics*, vol. 56, no. 2, pp. 1010–1017, May 2010. [Article \(CrossRef Link\)](#)
- [13] O. Lee, J. Bonnin, I. You, and T. Chung, "Comparative handover performance analysis of IPv6 mobility management protocols," *IEEE Transactions on Industrial Electronics*, vol. 60, no. 3, pp. 1077-1088, March 2013. [Article \(CrossRef Link\)](#)
- [14] L. J. Zhang and S. Pierre, "Performance analysis of fast handover for hierarchical MIPv6 in cellular networks," in *Proc. of IEEE 67th Vehicular Technology Conference (VTC2008-Spring)*, Marina Bay, Singapore, pp. 2374- 2378, May 2008. [Article \(CrossRef Link\)](#)
- [15] H. Nashaat, R. Rizk and H. Mahdi, "An analytical framework of fast handover for hierarchical MIPv6," in *Proc. of the World Congress on Computer Science and Information Technology (WCSIT'11)*, vol. 1, no. 2, pp. 38- 44, Egypt, January 2011. [Article \(CrossRef Link\)](#)
- [16] C. Makaya and S. Pierre, "An analytical framework for performance evaluation of IPv6-based mobility management protocols," *IEEE Transactions on Wireless Communication*, vol. 7, no. 3, pp. 972–983, March 2008. [Article \(CrossRef Link\)](#)
- [17] M. Skorepa, and R. Klug, "Enhanced analytical method for IP mobility handover schemes cost evaluation," *Telecommunication Systems*, vol. 52, no. 3, pp. 1573-1582, March 2013. [Article \(CrossRef Link\)](#)
- [18] H. S. Yoo, R. Tolentino, B. Park, B. Y. Chang, and S .H . Kim, "ES-FHMIPv6: An efficient scheme for fast handover over HMIPv6 networks," *International Journal of Future Generation Communication and Networking*, vol. 2, no. 2, pp. 38-48, June 2009.
[Article \(CrossRef Link\)](#)
- [19] V. B. Hency, J. Christina, A. Dhushanthini, V. T. Aiswariya , and D.Sridharan "An enhanced fast handover using hierarchical setup for mobile IP," *International Journal of Engineering and Technology (IJET)*, vol. 1, no. 3, pp. 213- 218, August 2009. [Article \(CrossRef Link\)](#)
- [20] L. J. Zhang and S. Pierre, "Evaluating the performance of fast handover for hierarchical MIPv6 in cellular networks," *Journal of Networks*, vol. 3, no. 6, pp. 36-43, 2008.
[Article \(CrossRef Link\)](#)
- [21] C. Makaya, S. Pierre, "An analytical framework for performance evaluation of IPv6-based mobility management protocols," *IEEE Transaction Wireless Communication*, vol. 7, no. 3, pp. 972- 983, 2008. [Article \(CrossRef Link\)](#)

- [22] L. Yun, Z. Yi-sheng, L. Qi-lie and W. Feng, "Performance research of MIPv6 and extended protocols in the process of handover," in *Proc. of International Conference on Wireless Communications, Networking and Mobile Computing - WiCom*, China, 2009. [Article \(CrossRef Link\)](#)
- [23] S. Gambhir, "A novel approach to reduce signaling delay in HMIPv6 mobile networks," *International Journal of Engineering and Technology*, vol. 1, no. 1, pp. 34-39, April 2009. [Article \(CrossRef Link\)](#)
- [24] H. Tuncer, S. Mishra, N. Shenoy, "A survey of identity and handover management approaches for the future Internet," *Sciencedirect in Computer Communications*, vol. 36, pp. 63-79, 2012. [Article \(CrossRef Link\)](#)
- [25] S. Matinkhah, S. Khorsandi1, and S.Yarahmadian,"A new handover management system for heterogeneous wireless access networks," *International Journal of Communication Systems*, vol. 27, no. 7, pp. 1020-1033, July 2014. [Article \(CrossRef Link\)](#)
- [26] C. Makaya and S. Pierre S, "An analytical framework for performance evaluation of IPv6-based mobility management protocols," *IEEE Transactions on wireless communications*, vol. 7, no. 3, pp. 972-983, 2008. [Article \(CrossRef Link\)](#)
- [27] V. Casares-Giner, V. Pla, and P. Escalle-Garcia, "Mobility models for mobility management," *Springer LNCS 5233*, pp. 716-745, 2011. [Article \(CrossRef Link\)](#)
- [28] H. Su-Cheng, L. Chien-Sing and N. Mustapha, "Bridging XML and relational databases: mapping choices and performance evaluation," *IETE Technical review*, vol. 27, no. 4, July-August 2010. [Article \(CrossRef Link\)](#)
- [29] V. Gupta and S. Dharmaraja, "Reliability and performance modeling of VoIP system with multiple component failure," *International Journal of Reliability and Safety*, 2011. [Article \(CrossRef Link\)](#)



Heba Nashaat is an assistant professor in the Electrical Engineering Department, Port Said University, Egypt. She received her B.Sc. and M.Sc. degrees in computer and control engineering, Suez Canal University, in 2001 and 2006, respectively. Her Ph.D. degree in computer and control engineering is received from Port Said University in 2011. Her research interests are in the area of computer networking, including mobile networks, handovers, and cloud computing. She is the executive director of Network Infrastructure, Port Said University.



Rawya Rizk is an associate professor at the Electrical Engineering Department, Port Said University, Egypt. She received her B.Sc., M.Sc. and Ph.D. in Computer and Control Engineering from Suez Canal University in 1991, 1996 and 2001, respectively. Her research interests are in computer networking, including mobile networking, wireless networks, sensor networks, ad hoc networks, QoS, routing, traffic and congestion control, handovers and cloud computing. She is the Chief Information Officer (CIO), Port Said University.